Mass Spectrometric Analysis of Intact Lipooligosaccharide: Direct Evidence for *O*-Acetylated Sialic Acids and Discovery of *O*-Linked Glycine Expressed by *Campylobacter jejuni*†

Monika Dzieciatkowska,‡ Denis Brochu,‡ Alex van Belkum,§ Astrid P. Heikema,§ Nobuhiro Yuki,|| R. Scott Houliston,‡ James C. Richards,‡ Michel Gilbert,*,‡ and Jianjun Li*,‡

Institute for Biological Sciences, National Research Council Canada, Ottawa, Ontario, Canada K1A 0R6, Department of Medical Microbiology and Infectious Diseases, Erasmus University Medical Center, Rotterdam, The Netherlands, and Department of Neurology and Research Institute of Neuroimmunological Diseases, Dokkyo Medical University School of Medicine, Tochigi, Japan

Received June 21, 2007; Revised Manuscript Received September 12, 2007

ABSTRACT: The lipooligosaccharides (LOS) of *Campylobacter jejuni* is an important virulence factor. Its core oligosaccharide component is frequently sialylated and bears a close resemblance with host gangliosides. The display of ganglioside mimics by this bacterium is believed to trigger the onset of the autoimmune condition Guillain-Barré syndrome (GBS) in some individuals. Considerable effort has been directed toward the structural characterization of the glycan component of the LOS of *C. jejuni* strains isolated from GBS patients. Capillary electrophoresis−mass spectrometry (CE−MS) has been a particularly useful analytical technique applied toward this task. Conventional analysis of bacterial LOS by CE−MS has generally involved the prior removal of *O*-acyl lipid chains, which is necessary for the effective solubilization and separation of the heterogeneous ensemble of LOS species. Unfortunately, *O*-deacylation causes the undesired removal of important glycan-associated *O*-linked modifications, such as *O*-acetate and *O*-linked amino acids. In this report, we describe a CE−MS technique developed for the rapid analysis of fully intact LOS from *C. jejuni*. Using this method, we report the structural characterization of the glycan from 10 GBS-associated strains and two enteritis strains, using material isolated from as little as one colony. The application of this technique has enabled us to unambiguously identify LOS-bound *O*-acetylated sialic acid in a number of strains and has revealed for the first time that *C. jejuni* frequently modifies its core with *O*-linked glycine. Our studies demonstrate that MS-based structural analysis of bacterial LOS can be optimized to the level where only a single-colony quantity of material is required and time-consuming chemical treatments can be avoided.

As the leading cause of bacterial diarrhea disease worldwide, *Campylobacter jejuni* is widely recognized as an important enteric pathogen (*1*−*3*). The glycan component of its lipooligosaccharide (LOS)[1] often resembles the structure of host gangliosides, which are abundantly expressed in nerve cell membranes (*4*−*6*). This form of molecular mimicry is believed to elicit the production of autoreactive immunoglobulins that cross-react with nerve cell gangliosides, leading to the autoimmune condition Guillain-Barré syndrome (GBS) (*7*, *8*), and its clinical variant Fisher syndrome (FS) (*9*). There is an ongoing need for the development of rapid and accurate analytical techniques for the characterization of the LOS from *C. jejuni* strains isolated from GBS and FS patients.

The LOS of *C. jejuni* is composed of two covalently linked domains: the hydrophobic anchor lipid A and the oligosaccharide, which consists of a conserved inner core and a variable outer core. The chemical structure of the lipid A component of the LOS from *C. jejuni* was elucidated previously (*10*, *11*). In most strains, the disaccharide backbone consists of a β-D-GlcN3N-(1→6)-α-D-GlcN (2,3-diamino-2,3-dideoxy-D-glucose and D-glucosamine) unit substituted with phosphomonoester groups at O-1 and O-4′. Typically, lipid A is acylated with primary 3-hydroxytetradecanoic acid 14:0(3-OH) at N-2, N-2′, and N-3′ and at O-3 via amide and ester linkages, respectively, and secondary hexadecanoic acid 16:0 at positions N-2′ and N-3′. The disaccharide backbone in a minority of strains was found to be either β-D-GlcN3N-(1→6)-α-D-GlcN3N or β-D-GlcN-(1→6)-α-D-GlcN. The LOS inner core contains two L-α-D-

† This study was supported by a grant from the Human Frontier Science Program (RGP 38/2003).

* To whom correspondence should be addressed. J.L.: telephone, (613) 990-0558; fax, (613) 952-9092; e-mail, Jianjun.Li@nrc-cnrc.gc.ca. M.G.: telephone, (613) 991-9956; fax, (613) 952-9092; e-mail, Michel.Gilbert@nrc-cnrc.gc.ca.

‡ National Research Council Canada.

§ Erasmus University Medical Center.

|| Dokkyo Medical University School of Medicine.

[1] Abbreviations: LOS, lipooligosaccharide; Hep, L-*glycero*-D-*manno*-heptose; KDO, 3-deoxy-D-*manno*-oct-2-ulosonic acid; Neu5Ac, *N*-acetylneuraminic acid; Hex, hexose; Gal, galactose; Glc, glucose; GalNAc, *N*-acetylgalactosamine; GlcN, 2-amino-2-deoxy-D-glucose; GlcN3N, 2,3-diamino-2,3-dideoxy-D-glucose; *P*, phosphate; *P*Etn, phosphoethanolamine; *PP*Etn, pyrophosphoethanolamine; Ac, acetate; Gly, glycine; SOAT, sialate *O*-acetyltransferase; GBS, Guillain-Barré syndrome; FS, Fisher syndrome.

10.1021/bi701229k CCC: $37.00
Published on Web 11/23/2007

Hep residues attached to a 2-keto-3-deoxyoctulosonic acid (KDO) residue, forming a conserved trisaccharide of L-α-D-Hep-(1→3)-L-α-D-Hep-(1→5)-KDO. The heptose attached to KDO is substituted at position 6 with either phosphate (*P*) or phosphoethanolamine (*P*Etn). In contrast to the conserved nature of the inner core, the outer core is more variable, consisting of various combinations of *N*-acetylhexosamine and hexose residues, and often 5-*N*-acetylneuraminic acid (Neu5Ac), linked terminally or subterminally to galactose (*12*−*17*). Some strains possess disialate residues, where terminal Neu5Ac is α2−8-linked to subterminal Neu5Ac (*13*, *16*). The addition of sialic acid to the LOS is catalyzed by either sialyltransferase Cst-II or Cst-III (*18*). Depending on the allelic variant carried by the strain, Cst-II can possess either monofunctional α2−3 transferase activity or α2−3/α2−8 bifunctional transferase activity (*19*). Cst-III is always monofunctional, i.e., with only α2−3 transferase activity. The sialylated core oligosaccharide structures displayed by many *C. jejuni* strains resemble human gangliosides. For instance, Aspinall et al. (*17*) reported that *C. jejuni* serotypes HS:1, HS:23, and HS:36 possess a GM2-like structure, whereas *C. jejuni* HS:41 was found to have a structure resembling GM1a (*15*). Mimicry of the disialosyl-containing ganglioside GD3 has also been reported in strain HS:10 (*16*).

O-Acetylation of sialic acids is a biologically significant modification and has been implicated in a growing number of physiological and pathological processes (*20*, *21*). Several bacteria have been shown to *O*-acetylate capsule-bound Neu5Ac, resulting in altered immunogenicity and susceptibility to glycosidases (*22*−*24*). We recently demonstrated that several *C. jejuni* strains carry a sialate *O*-actyltransferase (SOAT), which targets LOS-bound Neu5Ac, with a high specificity for terminal α2,8-linked residues (*25*). The SOAT gene, which was recombinantly expressed in *Escherichia coli*, is soluble and homologous with members of the NodL-LacA-CysE family of *O*-acetyltransferases. The presence of LOS-bound *O*-acetyl-Neu5Ac was detected indirectly, following enzymatic cleavage from whole cells, and subsequent analysis of cell-free extracts.

In the past, CE−MS characterization of the LOS from *C. jejuni* has been limited to the use of *O*-deacylated or more infrequently acid-cleaved species (*26*). While providing valuable structural insight into the backbone structure of the core glycan, these chemical treatments caused important glycan-associated *O*-linked or acid-sensitive moieties to be lost, rendering their detection inaccessible with this technique. In this work, we report the application of a highly sensitive electrophoresis-assisted open-tubular liquid chromatography−mass spectrometry (EA-OTLC−MS) approach to the analysis of intact LOS from *C. jejuni*, which has obviated the need for the *O*-deacylation procedure and, in so doing, has provided important insight into the presence of LOS-bound *O*-linked acetate and glycine modifications in this organism.

MATERIALS AND METHODS

Bacterial Strains and LOS Isolation. The *C. jejuni* HS:19 serostrain (ATCC 43446) and HB93-13 (ATCC 700297) were obtained from the American Type Culture Collection. *C. jejuni* strains OH4382 and OH4384 were obtained from the Laboratory Center for Disease Control (Health Canada, Winnipeg, MB). Strains MF6, GB11, GB16, GB19, and GB26 were described by Godschalk et al. (*8*). Strains GC033 and GC175 were described by Takahashi et al. (*27*). *C. jejuni* NCTC 11168 (HS:2) was originally isolated from a case of human enteritis (*28*) and later sequenced by Parkhill et al. (*29*). The *C. jejuni* GB11 *orf11* mutant was described by Godschalk et al. (*1*).

C. jejuni strains were cultured for 24−48 h on Mueller-Hinton agar plates in a microaerobic atmosphere at 37 °C. The cells were recovered by washing the colonies from the plates and dispersing them in 300 μL of phosphate-buffered saline (pH 7.4), which was further diluted with 700 μL of 100% ethanol to a final concentration of 70% ethanol. The cells were incubated at room temperature for 1 h, pelleted (16000*g* for 2 min), washed twice with ethanol followed by two washes with acetone, and finally air-dried overnight. The dried cells were dissolved in 200 μL of deionized water to which a 6 μL aliquot of proteinase K (2 mg/mL) had been added. The suspended cell solutions were incubated at 37 °C for 4 h, and the digestion was stopped by increasing the temperature to 75 °C for 10 min. The solutions were allowed to cool at room temperature and were subsequently freeze-dried. The cells were resuspended in a 200 μL solution of 20 mM ammonium acetate buffer (pH 7.5) containing DNase (100 μg/mL) and RNase (200 μg/mL) and incubated at 37 °C for 6 h before lyophilization. The digested cells were resuspended in 200 μL of deionized water. Following ultracentrifugation (436000*g* at 4 °C for 1 h), the LOS pellets were redissolved in water and lyophilized.

Preparation of Oligosaccharides: Mild Acid Hydrolysis of LOS. The core oligosaccharide was isolated following mild acid hydrolysis of the LOS (1.5% acetic acid at 100 °C for 2 h). The reaction mixture was cooled, and the insoluble lipid A was removed by centrifugation. The carbohydrate-containing supernatant was lyophilized and investigated by CE−MS.

Capillary Electrophoresis−Electrospray Mass Spectrometry. CE−MS was performed using a Prince CE system (Prince Technologies) coupled to a 4000 QTRAP mass spectrometer (Applied Biosystems/MDS Sciex). A sheath solution (2:1 2-propanol/methanol) was delivered at a flow rate of 1.0 μL/min. Separations were obtained on an ∼90 cm long bare fused-silica capillary using 15 mM ammonium acetate in deionized water (pH 9.0) or 30 mM morpholine in deionized water (pH 9.0). A separation voltage of 20 kV, together with a pressure of 500 mbar, was used for fast CE−MS analysis. The 5.2 and −5.2 kV electrospray ionization voltages were used for positive ion mode and negative ion mode detections, respectively.

Electrophoresis-Assisted Open-Tubular Liquid Chromatography−Mass Spectrometry. LOS samples were washed with methanol (3 × 100 μL) with vigorous stirring. The insoluble material was collected after centrifugation and suspended in 30 μL of water. Typically, 1.0 μL of LOS was applied to the capillary column followed by a wash with 1.0 μL of methanol. A small plug (60 nL) of 1.0 M ammonium acetate in deionized water was injected to elute the adsorbed LOS from the capillary surface. The separation was performed using 30 mM morpholine in deionized water (pH 9.0). A separation voltage of 20 kV, together with a pressure of 500 mbar, was applied for the EA-OTLC−MS analysis. The ESI voltage applied on the sprayer was set at

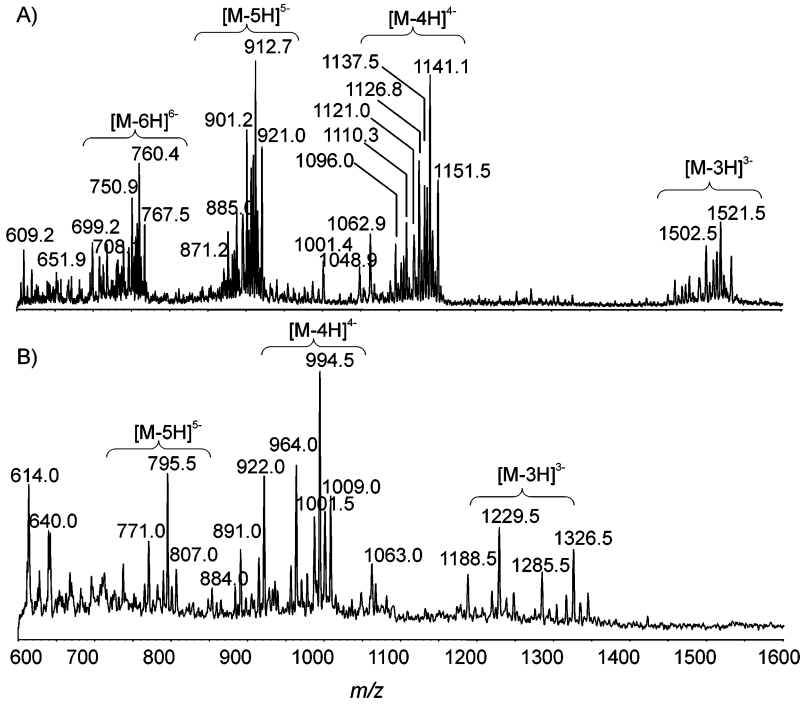

FIGURE 1: Negative ion MS analysis of intact LOS from *C. jejuni*: (A) strain GB19 and (B) strain OH4382.

−5.2 kV. Data acquisition was performed in the range of *m*/*z* 600−2000 at a scan rate of 2 s/spectrum.

For all MS experiments, nitrogen was used as the curtain gas and collision gas. In the MS/MS (enhanced product ion scan or EPI) and MS^3 experiments, the scan speed was set to 4000 Da/s, with Q_0 trapping. In MS/MS and MS^3 experiments, the trap fill time was set as "dynamic" and the resolution of Q_1 was set as "unit". For MS^3 experiments, the excitation coefficient was set at a value to excite only the first isotope for a single charged precursor with the excitation time set to 100 ms.

RESULTS

MS Analysis of Intact LOS. Intact LOS samples from 13 (when including the GB11 *orf11* mutant) *C. jejuni* strains were analyzed using EA-OTLC−MS. Two representative mass spectra are shown in Figure 1, in which a series of triply, quadruply, and pentuply deprotonated ions were observed for intact LOS of *C. jejuni* strains GB19 (panel A) and OH4382 (panel B). The MS spectrum of the LOS from *C. jejuni* GB19 was consistent with a heterogeneous mixture of disialylated glycoforms in which much of the variability was attributed to the presence or absence of glycyl (Gly), acetyl (Ac), and phosphoryl (*P*Etn) modifications. For example, the quadruply charged ions at *m*/*z* 1096.0, 1110.3, 1126.8, and 1141.1 correspond to species with the compositions $Neu5Ac_2{\cdot}Hex_4{\cdot}HexNAc_1{\cdot}Hep_2{\cdot}PEtn_1{\cdot}KDO_2{\cdot}$lipid A (*PP*Etn, *P*), Gly·$Neu5Ac_2{\cdot}Hex_4{\cdot}HexNAc_1{\cdot}Hep_2{\cdot}PEtn_1{\cdot}KDO_2{\cdot}$lipid A (*PP*Etn, *P*), $Neu5Ac_2{\cdot}Hex_4{\cdot}HexNAc_1{\cdot}Hep_2{\cdot}PEtn_1{\cdot}KDO_2{\cdot}$lipid A (*PP*Etn, *PP*Etn), and Gly·$Neu5Ac_2{\cdot}Hex_4{\cdot}HexNAc_1{\cdot}Hep_2{\cdot}PEtn_1{\cdot}KDO_2{\cdot}$lipid A (*PP*Etn, *PP*Etn), respectively. Structurally related glycoforms possessing a single *O*-acetyl modification were observed at *m*/*z* 1106.5, 1121.0, 1137.5, and 1151.5. For intact LOS from *C. jejuni* OH4382 (Figure 1B), quadruply charged ions were observed at *m*/*z* 891.0/964.0, 922.0/994.5, and 1009.0, corresponding to $Neu5Ac_{1\text{-}2}{\cdot}Hex_2{\cdot}Hep_2{\cdot}PEtn_1{\cdot}KDO_2{\cdot}$lipid A (*PP*Etn, *P*), $Neu5Ac_{1-2}{\cdot}Hex_2{\cdot}Hep_2{\cdot}PEtn_1{\cdot}KDO_2{\cdot}$lipid A (*PP*Etn, *PP*Etn), and Gly·$Neu5Ac_2{\cdot}Hex_2{\cdot}Hep_2{\cdot}PEtn_1{\cdot}KDO_2{\cdot}$lipid A (*PP*Etn, *P*), respectively. The absence of *O*-acetylated Neu5Ac in OH4382 is consistent with the presence of an inactive version of the SOAT gene in this strain (see below and ref *25*).

Characterization of Sialylation of LOS. To obtain structural information related specifically to the presence of *O*-acetylated glycoforms in *C. jejuni* GB19, tandem mass spectrometry experiments were carried out on the quadruply charged ions at *m*/*z* 1141.1 and 1151.5, and the spectra are presented in panels A and B of Figure 2, respectively. The fragment ions at *m*/*z* 290.2 and 581.3 give evidence for the presence of monosialic acid (Neu5Ac) and disialic acid (Neu5Ac-Neu5Ac), respectively. The fragment ion at *m*/*z* 332.2, corresponding to *O*-acetylated Neu5Ac, and the fragment ion at *m*/*z* 623.3, corresponding to the additional attachment of Neu5Ac, were observed in the tandem mass spectrum of ion at *m*/*z* 1151.5. These observations clearly indicated that the terminal Neu5Ac was *O*-acetylated. The tandem MS data also provide information about the composition of lipid A (e.g., doubly charged ions at *m*/*z* 1001.2 and 1062.7), differentiated by an additional phosphoethanolamine group (*P*Etn).

The combined MS and MS/MS data were then used to derive the molecular weights and compositions of different glycoforms, which are summarized in Table 1. The data revealed that each glycoform consisted of a conserved *P*Etn-substituted di-L-*glycero*-D-*manno*-heptosyl inner core moiety, attached via KDO to lipid A. The MS data are consistent with the lipid A portion of the molecule, consisting of a hybrid backbone of β-D-GlcN3N-(1→6)-α-D-GlcN carrying negative charged groups, *P* and *PP*Etn, at positions O-1 and O-4′ and substituted with six fatty acid chains [four 14:0(3-OH) and two 16:0] as amide and ester linkages.

Characterization of Acetylation of Sialic Acids in LOS. The LOS sialylation and corresponding *O*-acetylation can be screened using precursor ion monitoring MS experiments

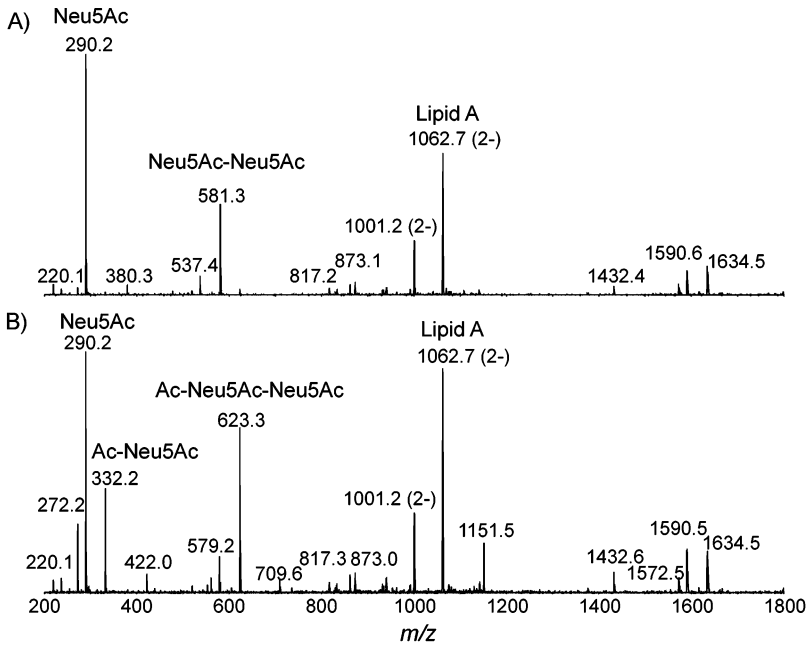

FIGURE 2: MS/MS analysis of intact LOS from *C. jejuni* GB19. (A) Extracted MS/MS spectrum of the ion at *m*/*z* 1141.1, corresponding to a composition of Gly·Neu5Ac$_2$·Hex$_4$·HexNAc$_1$·Hep$_2$·*P*Etn$_1$·KDO$_2$·lipid A (*PP*Etn, *PP*Etn). (B) Extracted MS/MS spectrum of the ion at *m*/*z* 1151.5, corresponding to a composition of Ac·Gly·Neu5Ac$_2$·Hex$_4$·HexNAc$_1$·Hep$_2$·*P*Etn$_1$·KDO$_2$·lipid A (*PP*Etn, *PP*Etn).

with a precursor at *m*/*z* 290.1 (Neu5Ac) or *m*/*z* 332.2 (Ac-Neu5Ac). The extracted precursor ion scan mass spectra (*m*/*z* 290.1) for strain GB19 and OH4382 are presented in panels A and E of Figure 3, respectively. The quadruply and pentuply deprotonated ions related to disialylated glycoforms containing glycine residues were observed in the extracted mass spectra. For strain GB19, the major ion at *m*/*z* 913.0/1141.0 corresponds to the glycine-subsituted disialylated glycoform Gly·Neu5Ac$_2$·Hex$_4$·HexNAc$_1$·Hep$_2$·*P*Etn$_1$·KDO$_2$·lipid A (*PP*Etn, *PP*Etn). A nonglycylated species was observed at *m*/*z* 901.5 ([M − 5H]$^{5-}$) and *m*/*z* 1127.0 ([M − 4H]$^{4-}$). The disialylated glycoforms lacking a *P*Etn moiety were detected at *m*/*z* 877.0/1096.5 and 888.5/1110.5. The precursor ion spectrum of *m*/*z* 290.1 for strain OH4382 gives prominent quadruply and pentuply deprotonated ions for the major disialylated glycoforms (Figure 3E). Disialylated glycoforms in GB19 and OH4382 were confirmed by scanning for the diagnostic ion at *m*/*z* 581.2 (Figure 3B,F). The spectra revealed that both strains contain disialylated glycoforms.

In full MS spectra, ions corresponding to *O*-acetylated Neu5Ac-containing glycoforms were not readily identified due to extensive overlap of signals from species corresponding to the major sialylated glycoforms and, in some cases, due to the low abundance of these species. However, their presence could be easily confirmed by selecting the ion at *m*/*z* 332.1 as a precursor, which corresponds to deprotonated *O*-acetylsialic acid (Figure 3C). As expected, the ions corresponding to O-acetylated Neu5Ac-containing species were observed only in the spectrum of intact LOS of *C. jejuni* GB19 (compare panels C and G of Figure 3). The presence of the *O*-acetylated disialic acid in the LOS was confirmed in a precursor ion monitoring experiment by selecting the ion at *m*/*z* 623.2 (Ac-Neu5Ac-Neu5Ac) as a precursor. Glycoforms containing *O*-acetyl-Neu5Ac-Neu5Ac were observed at *m*/*z* 1151.5 [M − 4H]$^{4-}$ and 1535.5 [M − 3H]$^{3-}$ (Figure 3D). The precursor ion scan experiments also revealed no *O*-acetylated Neu5Ac residues in the LOS of strain OH4382 (Figure 3H).

Correlation of the SOAT and Cst-II Activities with the Observed Sialylation and Acetylation Patterns. We previously reported that *C. jejuni* could have either mono- or bifunctional variants of Cst-II and active or inactive variants of the SOAT (*19*, *25*), when these genes are present. LOS-bound acetylated Neu5Ac requires the presence of a bifunctional Cst-II because the SOAT can transfer to only a Neu5Ac residue that is α2,8-linked to a subterminal Neu5Ac. In Table 2, we summarize the information known about the Cst-II and SOAT (*orf11*) variants for the 13 strains used in this study. We observed LOS-bound acetylated Neu5Ac in the five strains that have both a bifunctional Cst-II and an active *O*-acetyltransferase (MF6, GB16, GB19, GC033, and HB93-13). Two strains (OH4382 and OH4384) have a bifunctional Cst-II and an inactive SOAT, while four strains (GB11, GB26, GC175, and ATCC 43446) have an active SOAT but a predicted monofunctional Cst-II. Acetylated Neu5Ac glycoforms were not observed for four (OH4382, OH4384, GB26, and GC175) of these six strains (Table 1). We observed a trace amount of disialylated glycoforms in strains GB11 and ATCC 43446 which is surprising since they have a monofunctional Cst-II. We also observed small amounts of O-acetylated Neu5Ac-containing glycoforms in GB11 and ATCC 43446, which is consistent with the presence of an active *O*-acetyltransferase that targets those glycoforms that are disialylated. In these two strains, it is possible that Cst-II has a low level of bifunctional activity that allows the expression of trace amounts of disialylated species. The intact LOS of the GB11 *orf11* mutant (SOAT negative) had small amounts of disialylated glycoforms but no *O*-acetylated Neu5Ac-containing glycoforms (Table 1), which confirms the role of *orf11* in the acetylation of LOS-bound Neu5Ac. We have also analyzed one strain (NCTC 11168) that carries a monofunctional sialyltransferase (Cst-III instead of Cst-II) and does not carry the SOAT gene

Table 1: Proposed Compositions of Intact LOSs Based on MS and MS/MS Results

strain	observed ions (*m/z*)			molecular mass (Da)		relative abundance	proposed composition
	$[M-5H]^{5-}$	$[M-4H]^{4-}$	$[M-3H]^{3-}$	observed	calculated[a]		
GB16	876.7	1096.0	1461.6	4388.1	4386.5	0.9	Neu5Ac$_2$·Hex$_4$·HexNAc$_1$·Hep$_2$·*P*Etn$_1$·KDO$_2$·lipid A (*PP*Etn, *P*)
	885.3	1106.9	1475.5	4430.9	4428.6	0.4	Ac·Neu5Ac$_2$·Hex$_4$·HexNAc$_1$·Hep$_2$·*P*Etn$_1$·KDO$_2$·lipid A (*PP*Etn, *P*)
	888.1	1110.3	1480.5	4445.1	4443.6	0.6	Gly·Neu5Ac$_2$·Hex$_4$·HexNAc$_1$·Hep$_2$·*P*Etn$_1$·KDO$_2$·lipid A (*PP*Etn, *P*)
	897.1	1121.1	1494.7	4488.7	4486.6	0.2	Ac·Gly·Neu5Ac$_2$·Hex$_4$·HexNAc$_1$·Hep$_2$·*P*Etn$_1$·KDO$_2$·lipid A (*PP*Etn, *P*)
	901.3	1126.8	1502.5	4511.1	4509.6	1.0	Neu5Ac$_2$·Hex$_4$·HexNAc$_1$·Hep$_2$·*P*Etn$_1$·KDO$_2$·lipid A (*PP*Etn, *PP*Etn)
	910.0	1137.4	1516.7	4553.9	4551.6	0.5	Ac·Neu5Ac$_2$·Hex$_4$·HexNAc$_1$·Hep$_2$·*P*Etn$_1$·KDO$_2$·lipid A (*PP*Etn, *PP*Etn)
	912.9	1141.0	1521.5	4568.3	4566.6	0.7	Gly·Neu5Ac$_2$·Hex$_4$·HexNAc$_1$·Hep$_2$·*P*Etn$_1$·KDO$_2$·lipid A (*PP*Etn, *PP*Etn)
	921.1	1151.5	1535.6	4610.1	4608.7	0.3	Ac·Gly·Neu5Ac$_2$·Hex$_4$·HexNAc$_1$·Hep$_2$·*P*Etn$_1$·KDO$_2$·lipid A (*PP*Etn, *PP*Etn)
MF6		1023.1	1364.8	4096.9	4095.3	0.3	Neu5Ac$_1$·Hex$_4$·HexNAc$_1$·Hep$_2$·*P*Etn$_1$·KDO$_2$·lipid A (*PP*Etn, *P*)
		1037.4	1383.3	4153.3	4152.3	0.3	Gly·Neu5Ac$_1$·Hex$_4$·HexNAc$_1$·Hep$_2$·*P*Etn$_1$·KDO$_2$·lipid A (*PP*Etn, *P*)
	876.7	1096.0	1461.4	4387.9	4386.5	0.9	Neu5Ac$_2$·Hex$_4$·HexNAc$_1$·Hep$_2$·*P*Etn$_1$·KDO$_2$·lipid A (*PP*Etn, *P*)
	885.5	1107.0	1476.0	4431.8	4428.6	0.4	Ac·Neu5Ac$_2$·Hex$_4$·HexNAc$_1$·Hep$_2$·*P*Etn$_1$·KDO$_2$·lipid A (*PP*Etn, *P*)
	888.1	1110.3	1480.6	4445.2	4443.6	0.9	Gly·Neu5Ac$_2$·Hex$_4$·HexNAc$_1$·Hep$_2$·*P*Etn$_1$·KDO$_2$·lipid A (*PP*Etn, *P*)
	897.0	1121.5	1495.0	4489.3	4486.6	0.3	Ac·Gly·Neu5Ac$_2$·Hex$_4$·HexNAc$_1$·Hep$_2$·*P*Etn$_1$·KDO$_2$·lipid A (*PP*Etn, *P*)
	901.3	1126.8	1502.5	4511.1	4509.6	0.99	Neu5Ac$_2$·Hex$_4$·HexNAc$_1$·Hep$_2$·*P*Etn$_1$·KDO$_2$·lipid A (*PP*Etn, *PP*Etn)
	910.0	1137.5	1517.0	4554.3	4551.6	0.4	Ac·Neu5Ac$_2$·Hex$_4$·HexNAc$_1$·Hep$_2$·*P*Etn$_1$·KDO$_2$·lipid A (*PP*Etn, *PP*Etn)
	912.7	1141.0	1521.5	4568.0	4566.6	1.0	Gly·Neu5Ac$_2$·Hex$_4$·HexNAc$_1$·Hep$_2$·*P*Etn$_1$·KDO$_2$·lipid A (*PP*Etn, *PP*Etn)
	921.5	1152.0	1536.0	4611.8	4608.7	0.3	Ac·Gly·Neu5Ac$_2$·Hex$_4$·HexNAc$_1$·Hep$_2$·*P*Etn$_1$·KDO$_2$·lipid A (*PP*Etn, *PP*Etn)
GB19	876.7	1096.0	1461.5	4388.0	4386.5	0.4	Neu5Ac$_2$·Hex$_4$·HexNAc$_1$·Hep$_2$·*P*Etn$_1$·KDO$_2$·lipid A (*PP*Etn, *P*)
	885.2	1106.5	1475.5	4430.2	4428.6	0.3	Ac·Neu5Ac$_2$·Hex$_4$·HexNAc$_1$·Hep$_2$·*P*Etn$_1$·KDO$_2$·lipid A (*PP*Etn, *P*)
	888.0	1110.2	1480.4	4444.7	4443.6	0.5	Gly·Neu5Ac$_2$·Hex$_4$·HexNAc$_1$·Hep$_2$·*P*Etn$_1$·KDO$_2$·lipid A (*PP*Etn, *P*)
	896.0	1121.0	1494.5	4486.5	4486.6	0.4	Ac·Gly·Neu5Ac$_2$·Hex$_4$·HexNAc$_1$·Hep$_2$·*P*Etn$_1$·KDO$_2$·lipid A (*PP*Etn, *P*)
	901.2	1126.8	1502.4	4510.8	4509.6	0.8	Neu5Ac$_2$·Hex$_4$·HexNAc$_1$·Hep$_2$·*P*Etn$_1$·KDO$_2$·lipid A (*PP*Etn, *PP*Etn)
	910.0	1137.5	1516.5	4553.8	4551.6	0.7	Ac·Neu5Ac$_2$·Hex$_4$·HexNAc$_1$·Hep$_2$·*P*Etn$_1$·KDO$_2$·lipid A (*PP*Etn, *PP*Etn)
	912.7	1141.0	1521.4	4567.9	4566.6	1.0	Gly·Neu5Ac$_2$·Hex$_4$·HexNAc$_1$·Hep$_2$·*P*Etn$_1$·KDO$_2$·lipid A (*PP*Etn, *PP*Etn)
	921.1	1151.5	1535.1	4609.6	4608.7	0.6	Ac·Gly·Neu5Ac$_2$·Hex$_4$·HexNAc$_1$·Hep$_2$·*P*Etn$_1$·KDO$_2$·lipid A (*PP*Etn, *PP*Etn)
GC033	876.7	1096.0	1461.5	4388.0	4386.5	0.7	Neu5Ac$_2$·Hex$_4$·HexNAc$_1$·Hep$_2$·*P*Etn$_1$·KDO$_2$·lipid A (*PP*Etn, *P*)
	897.0	1121.0	1496.0	4489.7	4485.6	0.5	Ac·Gly·Neu5Ac$_2$·Hex$_4$·HexNAc$_1$·Hep$_2$·*P*Etn$_1$·KDO$_2$·lipid A (*PP*Etn, *P*)
	901.3	1126.8	1502.5	4511.1	4509.6	1.0	Neu5Ac$_2$·Hex$_4$·HexNAc$_1$·Hep$_2$·*P*Etn$_1$·KDO$_2$·lipid A (*PP*Etn, *PP*Etn)
		1137.5		4550.0	4551.6	0.1	Ac·Neu5Ac$_2$·Hex$_4$·HexNAc$_1$·Hep$_2$·*P*Etn$_1$·KDO$_2$·lipid A (*PP*Etn, *PP*Etn)
	912.7	1141.0	1521.6	4568.1	4566.6	0.8	Gly·Neu5Ac$_2$·Hex$_4$·HexNAc$_1$·Hep$_2$·*P*Etn$_1$·KDO$_2$·lipid A (*PP*Etn, *PP*Etn)
	921.5	1152.0		4612.3	4608.7	0.1	Ac·Gly·Neu5Ac$_2$·Hex$_4$·HexNAc$_1$·Hep$_2$·*P*Etn$_1$·KDO$_2$·lipid A (*PP*Etn, *PP*Etn)
HB93-13		891.2	1188.4	3568.5	3567.8	0.4	Neu5Ac$_1$·Hex$_2$·Hep$_2$·*P*Etn$_1$·KDO$_2$·lipid A (*PP*Etn, *P*)
	737.5	921.9	1229.7	3691.7	3690.9	1.0	Neu5Ac$_1$·Hex$_2$·Hep$_2$·*P*Etn$_1$·KDO$_2$·lipid A (*PP*Etn, *PP*Etn)
	748.9	936.2	1248.7	3748.8	3747.9	0.8	Gly·Neu5Ac$_1$·Hex$_2$·Hep$_2$·*P*Etn$_1$·KDO$_2$·lipid A (*PP*Etn, *PP*Etn)
	795.8	994.8	1326.8	3983.5	3982.1	0.9	Neu5Ac$_2$·Hex$_2$·Hep$_2$·*P*Etn$_1$·KDO$_2$·lipid A (*PP*Etn, *PP*Etn)
		1006.0	1340.5	4026.3	4024.2	0.1	Ac·Neu5Ac$_2$·Hex$_2$·Hep$_2$·*P*Etn$_1$·KDO$_2$·lipid A (*PP*Etn, *PP*Etn)
	807.2	1009.1	1345.8	4040.6	4039.2	0.8	Gly·Neu5Ac$_2$·Hex$_2$·Hep$_2$·*P*Etn$_1$·KDO$_2$·lipid A (*PP*Etn, *PP*Etn)
		1019.5	1360.0	4082.5	4081.2	0.1	Ac·Gly·Neu5Ac$_2$·Hex$_2$·Hep$_2$·*P*Etn$_1$·KDO$_2$·lipid A (*PP*Etn, *PP*Etn)
	863.0	1078.5	1437.5	4317.8	4315.4	0.1	Ac·Neu5Ac$_3$·Hex$_2$·Hep$_2$·*P*Etn$_1$·KDO$_2$·lipid A (*PP*Etn, *PP*Etn)
		1092.5	1457.0	4374.3	4372.5	0.1	Ac·Gly·Neu5Ac$_2$·Hex$_2$·Hep$_2$·*P*Etn$_1$·KDO$_2$·lipid A (*PP*Etn, *PP*Etn)
OH4382		891.0	1188.5	3568.3	3567.8	0.3	Neu5Ac$_1$·Hex$_2$·Hep$_2$·*P*Etn$_1$·KDO$_2$·lipid A (*PP*Etn, *P*)
		922.0	1229.5	3691.8	3690.7	0.5	Neu5Ac$_1$·Hex$_2$·Hep$_2$·*P*Etn$_1$·KDO$_2$·lipid A (*PP*Etn, *PP*Etn)
	771.0	964.0	1285.5	3859.8	3859.1	0.6	Neu5Ac$_2$·Hex$_2$·Hep$_2$·*P*Etn$_1$·KDO$_2$·lipid A (*PP*Etn, *P*)
	795.5	994.5	1326.5	3982.3	3982.1	1.0	Neu5Ac$_2$·Hex$_2$·Hep$_2$·PEtn$_1$·KDO$_2$·lipid A (*PP*Etn, *PP*Etn)
	807.0	1009.0	1345.5	4039.8	4039.2	0.5	Gly·Neu5Ac$_2$·Hex$_2$·Hep$_2$·*P*Etn$_1$·KDO$_2$·lipid A (*PP*Etn, *P*)
OH4384		982.7	1310.4	3934.5	3933.1	0.5	Neu5Ac$_1$·Hex$_3$·HexNAc$_1$·Hep$_2$·*P*Etn$_1$·KDO$_2$·lipid A (*PP*Etn, *P*)
		1013.5	1351.2	4057.3	4056.2	0.9	Neu5Ac$_1$·Hex$_3$·HexNAc$_1$·Hep$_2$·*P*Etn$_1$·KDO$_2$·lipid A (*PP*Etn, *PP*Etn)

[a] Isotope-averaged mass units were used for the calculation of molecular mass values based on proposed compositions as follows: Hex, 162.14; HexNAc, 203.19; Hep, 192.17; KDO, 220.18; *P*, 79.98; *P*Etn, 123.05; C14, 165.13; Neu5Ac, 291.26; Gly, 57.05; Ac, 42.03; 3-OH C14:0, 226.36; C16:0, 238.41; H_2O, 18.01.

Table 1: (Continued)

strain	observed ions (*m/z*)			molecular mass (Da)		relative abundance	proposed composition
	$[M-5H]^{5-}$	$[M-4H]^{4-}$	$[M-3H]^{3-}$	observed	calculated[a]		
OH4384	822.3	1027.5	1370.5	4115.0	4113.2	0.9	Gly·Neu5Ac$_1$·Hex$_3$·HexNAc$_1$·Hep$_2$·*P*Etn$_1$·KDO$_2$·lipid A (*PP*Etn, *PP*Etn)
	868.9		1448.3	4348.7	4347.5	0.2	Neu5Ac$_2$·Hex$_3$·HexNAc$_1$·Hep$_2$·*P*Etn$_1$·KDO$_2$·lipid A (*PP*Etn, *PP*Etn)
	902.4	1128.3	1504.5	4516.9	4515.7	0.4	Neu5Ac$_3$·Hex$_3$·HexNAc$_1$·Hep$_2$·*P*Etn$_1$·KDO$_2$·lipid A (*PP*Etn, *P*)
	927.0	1159.0	1545.4	4639.8	4638.7	1.0	Neu5Ac$_3$·Hex$_3$·HexNAc$_1$·Hep$_2$·*P*Etn$_1$·KDO$_2$·lipid A (*PP*Etn, *PP*Etn)
	938.4	1173.3	1564.6	4697.0	4695.8	0.8	Gly·Neu5Ac$_3$·Hex$_3$·HexNAc$_1$·Hep$_2$·*P*Etn$_1$·KDO$_2$·lipid A (*PP*Etn, *PP*Etn)
GB26	818.5	1023.1	1364.5	4096.8	4095.3	0.8	Neu5Ac$_1$·Hex$_4$·HexNAc$_1$·Hep$_2$·*P*Etn$_1$·KDO$_2$·lipid A (*PP*Etn, *P*)
	843.1	1053.9	1405.5	4219.9	4218.3	1.0	Neu5Ac$_1$·Hex$_4$·HexNAc$_1$·Hep$_2$·*P*Etn$_1$·KDO$_2$·lipid A (*PP*Etn, *PP*Etn)
	854.4	1068.2	1424.8	4277.1	4275.4	0.5	Gly·Neu5Ac$_1$·Hex$_4$·HexNAc$_1$·Hep$_2$·*P*Etn$_1$·KDO$_2$·lipid A (*PP*Etn, *PP*Etn)
GC175		891.2	1188.5	3568.6	3567.8	0.5	Neu5Ac$_1$·Hex$_2$·Hep$_2$·*P*Etn$_1$·KDO$_2$·lipid A (*PP*Etn, *P*)
		922.0	1229.7	3692.1	3690.9	1.0	Neu5Ac$_1$·Hex$_2$·Hep$_2$·*P*Etn$_1$·KDO$_2$·lipid A (*PP*Etn, *PP*Etn)
		936.3	1248.5	3748.8	3747.9	0.6	Gly·Neu5Ac$_1$·Hex$_2$·Hep$_2$·*P*Etn$_1$·KDO$_2$·lipid A (*PP*Etn, *PP*Etn)
11168		1063.7	1418.3	4258.4	4256.2	0.6	Neu5Ac$_1$·Hex$_5$·HexNAc$_1$·Hep$_2$·*P*Etn$_1$·Kdo$_2$·lipid A (*PP*Etn, *P*)
		1094.4	1459.2	4381.1	4379.2	1.0	Neu5Ac$_1$·Hex$_5$·HexNAc$_1$·Hep$_2$·*P*Etn$_1$·Kdo$_2$·lipid A (*PP*Etn, *PP*Etn)
		1135.0	1513.2	4543.3	4541.4	0.3	Neu5Ac$_1$·Hex$_6$·HexNAc$_1$·Hep$_2$·*P*Etn$_1$·Kdo$_2$·lipid A (*PP*Etn, *PP*Etn)
ATCC 43446 (HS:19)		982.4	1310.8	3934.5	3933.1	0.3	Neu5Ac$_1$·Hex$_3$·HexNAc$_1$·Hep$_2$·*P*Etn$_1$·KDO$_2$·lipid A (*PP*Etn, *P*)
		1013.4	1351.6	4057.7	4056.2	0.6	Neu5Ac$_1$·Hex$_3$·HexNAc$_1$·Hep$_2$·*P*Etn$_1$·KDO$_2$·lipid A (*PP*Etn, *PP*Etn)
	843.9	1055.6	1407.6	4225.6	4223.2	0.6	Neu5Ac$_2$·Hex$_3$·HexNAc$_1$·Hep$_2$·*P*Etn$_1$·KDO$_2$·lipid A (*PP*Etn, *P*)
	869.1	1085.9	1448.6	4348.9	4347.5	1.0	Neu5Ac$_2$·Hex$_3$·HexNAc$_1$·Hep$_2$·*P*Etn$_1$·KDO$_2$·lipid A (*PP*Etn, *PP*Etn)
	880.1	1100.3	1467.1	4405.0	4403.3	0.8	Gly·Neu5Ac$_2$·Hex$_3$·HexNAc$_1$·Hep$_2$·*P*Etn$_1$·KDO$_2$·lipid A (*PP*Etn, *PP*Etn)
	927.5	1159.2	1545.5	4640.9	4638.7	0.1	Neu5Ac$_3$·Hex$_3$·HexNAc$_1$·Hep$_2$·*P*Etn$_1$·KDO$_2$·lipid A (*PP*Etn, *PP*Etn)
	935.5	1169.5	1560.0	4682.5	4680.8	0.1	Ac·Neu5Ac$_3$·Hex$_3$·HexNAc$_1$·Hep$_2$·*P*Etn$_1$·KDO$_2$·lipid A (*PP*Etn, *PP*Etn)
	947.5	1184.5	1579.0	4740.8	4737.8	0.1	Ac·Gly·Neu5Ac$_3$·Hex$_3$·HexNAc$_1$·Hep$_2$·*P*Etn$_1$·KDO$_2$·lipid A (*PP*Etn, *PP*Etn)
GB11		982.6	1310.3	3934.1	3933.1	0.3	Neu5Ac$_1$·Hex$_3$·HexNAc$_1$·Hep$_2$·*P*Etn$_1$·KDO$_2$·lipid A (*PP*Etn, *P*)
		1013.3	1351.4	4057.2	4056.2	0.4	Neu5Ac$_1$·Hex$_3$·HexNAc$_1$·Hep$_2$·*P*Etn$_1$·KDO$_2$·lipid A (*PP*Etn, *PP*Etn)
	844.3	1055.4	1407.5	4225.9	4224.4	0.6	Neu5Ac$_2$·Hex$_3$·HexNAc$_1$·Hep$_2$·*P*Etn$_1$·KDO$_2$·lipid A (*PP*Etn, *P*)
	868.8	1086.1	1448.4	4348.5	4347.5	1.0	Neu5Ac$_2$·Hex$_3$·HexNAc$_1$·Hep$_2$·*P*Etn$_1$·KDO$_2$·lipid A (*PP*Etn, *PP*Etn)
	880.3	1100.4	1467.4	4405.8	4404.5	0.6	Gly·Neu5Ac$_2$·Hex$_3$·HexNAc$_1$·*P*Etn$_1$Hep$_2$·KDO$_2$·lipid A (*PP*Etn, *PP*Etn)
	927.5	1159.2	1545.5	4640.9	4638.7	0.1	Neu5Ac$_3$·Hex$_3$·HexNAc$_1$·Hep$_2$·*P*Etn$_1$·KDO$_2$·lipid A (*PP*Etn, *PP*Etn)
	936.0	1169.9	1560.0	4683.9	4680.8	0.1	Ac·Neu5Ac$_3$·Hex$_3$·HexNAc$_1$·Hep$_2$·*P*Etn$_1$·KDO$_2$·lipid A (*PP*Etn, *PP*Etn)
	947.5	1184.0	1579.0	4740.8	4737.8	0.1	Ac·Gly·Neu5Ac$_3$·Hex$_3$·HexNAc$_1$·Hep$_2$·*P*Etn$_1$·KDO$_2$·lipid A (*PP*Etn, *PP*Etn)
GB11 (o*rf11* mutant)		981.9	1310.4	3932.9	3933.1	0.4	Neu5Ac$_1$·Hex$_3$·HexNAc$_1$·Hep$_2$·*P*Etn$_1$·KDO$_2$·lipid A (*PP*Etn, *P*)
			1351.3	4056.9	4056.2	0.5	Neu5Ac$_1$·Hex$_3$·HexNAc$_1$·Hep$_2$·*P*Etn$_1$·KDO$_2$·lipid A (*PP*Etn, *PP*Etn)
		1055.1	1407.1	4224.3	4224.4	1.0	Neu5Ac$_2$·Hex$_3$·HexNAc$_1$·Hep$_2$·*P*Etn$_1$·KDO$_2$·lipid A (*PP*Etn, *P*)
		1086.3	1448.4	4348.7	4347.5	0.7	Neu5Ac$_2$·Hex$_3$·HexNAc$_1$·Hep$_2$·*P*Etn$_1$·KDO$_2$·lipid A (*PP*Etn, *PP*Etn)
		1100.1	1467.4	4404.8	4404.5	0.3	Gly·Neu5Ac$_2$·Hex$_3$·HexNAc$_1$·*P*Etn$_1$Hep$_2$·KDO$_2$·lipid A (*PP*Etn, *PP*Etn)
		1159.1	1545.3	4639.6	4638.7	0.1	Neu5Ac$_3$·Hex$_3$·HexNAc$_1$·Hep$_2$·*P*Etn$_1$·KDO$_2$·lipid A (*PP*Etn, *PP*Etn)

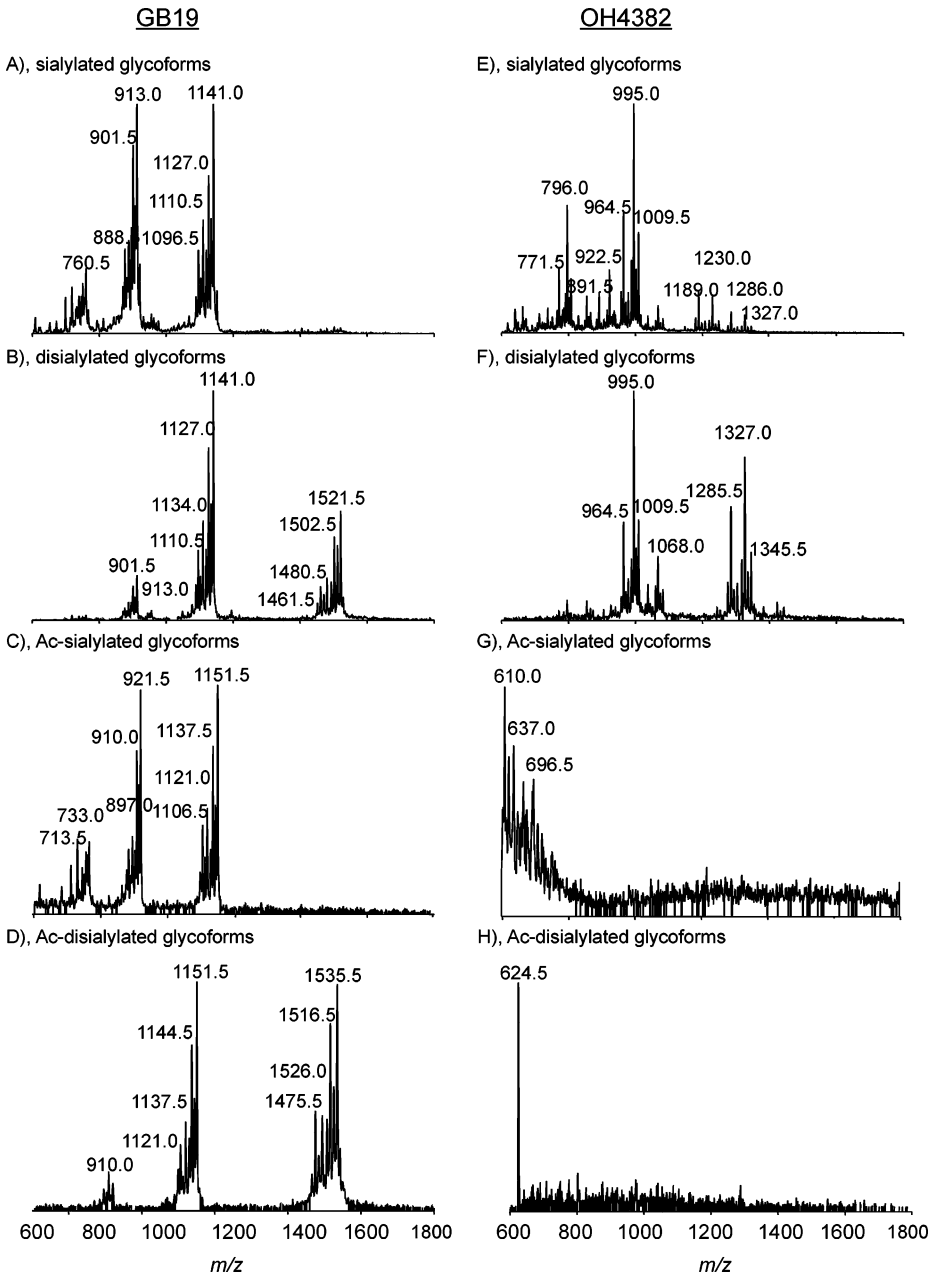

FIGURE 3: Precursor ion analysis of intact LOS from *C. jejuni* GB19 (A−D) and OH4382 (E−H). (A and E) Precursor ion mass spectrum of the ion at *m*/*z* 290.1. (B and F) Precursor ion mass spectrum of the ion at *m*/*z* 581.2. (C and G) Precursor ion mass spectrum of the ion at *m*/*z* 332.1. (D and H) Precursor ion mass spectrum of the ion at *m*/*z* 623.2.

(*orf11*). As expected, disialylated and *O*-acetylated Neu5Ac-containing glycoforms are absent in NCTC 11168. The EA-OTLC−MS technique is effective in analyzing material isolated from just one colony of cells, which was demonstrated through analysis of the MF6 strain (Supporting Information, Figure S1).

Location of the Glycine Residue in LOS. Although glycine has not been reported in *C. jejuni* LOS, the presence of this amino acid has been previously detected as a substituent in the LOS of other Gram-negative bacteria (*30*−*32*). To detect glycine and confirm its location within the glycan component of the LOS, MS^3 experiments on the sodiated ions were performed. Detailed structural information is summarized in Scheme 1, in which all strains comprise an anhydro-KDO moiety (*An*KDO-ol) formed during delipidation by β-elimination of the appended KDO group from C-4 of linking KDO as observed in previous studies (*33*). The mild acid conditions used for delipidation also remove the sialic acid groups.

The core oligosaccharide of *C. jejuni* strain NCTC 11168 is shown in Scheme 1. Interestingly, this is the only strain that was shown to have no glycine in its LOS (core 1). The oligosaccharide fractions of *C. jejuni* strains GB26, GB19, GC033, GB16, and MF6 were found to have the core 2 structure. A representative mass spectrum (*C. jejuni* GB19) revealed a single ion (*m*/*z* 1580.3) corresponding to the molecular mass of the core region (Figure 4A). In addition, we observed major ions with additional masses of 57 Da, corresponding to the glycinated analogues (*m*/*z* 1637.2). A series of sodiated ions were also observed (*m*/*z* 1602.1 and 1659.2). MS/MS analysis of the ion at *m*/*z* 1659.2 corresponding to sodiated core oligosaccharide with a single glycine residue attached is shown in Figure 4B. The spectrum showed a series of B-type ions (e.g., $B_{2\alpha}$ at *m*/*z* 388.3, $B_{3\alpha}$

Table 2: Variants of Sialate *O*-Acetyltransferase (SOAT encoded by *orf11*) and Sialyltransferase (Cst-II) Observed in the *C. jejuni* Strains that Were Analyzed for the Presence of *O*-Acetyl-Neu5Ac

strain	country[a]	disease[b]	GenBank entry: Cst-II	GenBank entry: Orf11	Cst-II variant[c]	predicted SOAT activity[d]	expected 9-*O*-acetyl-Neu5Ac[e]	observed 9-*O*-acetyl-Neu5Ac	comment
ATCC 43446 (HS:19)	Canada	enteritis	AF167344	AF167344	mono	+	−	−/+	trace amount of acetyl-Neu5Ac
GB11	The Netherlands	GBS	AY422197	AY422197	mono	+	−	−/+	trace amount of acetyl-Neu5Ac
GB11 (*orf11* mutant)	The Netherlands	GBS	AY422197	AY422197	mono	−	−	−	gene-specific knockout of *orf11* (SOAT) made by Godschalk et al. (*1*)
GB16	The Netherlands	GBS	EF076703	DQ357235	bi	+	+	+	phase-variable G-tract in *orf11*
GB19	The Netherlands	GBS	DQ357237	DQ357237	bi	+	+	+	phase-variable G-tract in *orf11*
GB26	The Netherlands	GBS	DQ351737	DQ351737	mono	+	−	−	
MF6	The Netherlands	FS	AY422196	AY422196	bi	+	+	+	phase-variable G-tract in *orf11*
HB93−13	China	GBS	AY297047	AY297047	bi	+	+	+	
GC033	Japan	FS	DQ536321	DQ354586	bi	+	+	+	phase-variable G-tract in *orf11*
GC175	Japan	GBS	DQ077811	DQ357247	mono	+	−	−	
OH4382	Japan	GBS	(AF130984)[f]	(AF130984)	bi	−	−	−	SOAT is inactive due to Asp75Gly mutation
OH4384	Japan	GBS	AF130984	AF130984	bi	−	−	−	SOAT is inactive due to Asp75Gly mutation
NCTC 11168	United Kingdom	enteritis	AL111168	absent	mono	−	−	−	has Cst-III (rather than Cst-II) and no SOAT

[a] The strains from The Netherlands are described by Godschalk et al. (*8*), while the isolates from Japan are described by Takahashi et al. (*27*). ATCC 43446 is the HS:19 Penner serostrain. [b] All of the strains came from patients who had enteritis. Some of the patients also developed neurological symptoms as indicated: GBS, Guillain-Barré syndrome; FS, Fisher syndrome. [c] Monofunctional Cst-II has α2,3 activity, and bifunctional Cst-II has both α2,3 and α2,8 activities (*18*). [d] Data for active or inactive SOAT (Orf11) variants are from Houliston et al. (*25*). [e] We expect to observe 9-*O*-acetyl-Neu5Ac when there is a combination of active SOAT and bifunctional Cst-II. [f] The sequences of Cst-II and Orf11 from OH4382 are identical to that from OH4384.

Scheme 1

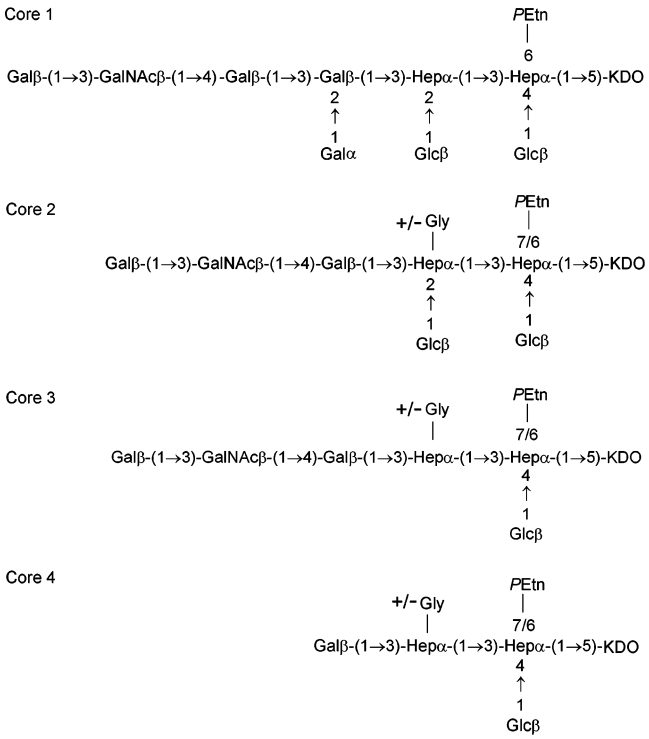

at *m*/*z* 550.2, and $B_{4\alpha}$ at *m*/*z* 961.3), along with the B_5 ions corresponding to consecutive losses of *P*Etn (B_5-123 or *m*/*z* 1315.6) and Hex (B_5-123−162 or *m*/*z* 1153.4). In addition, a series of C-type ions were also detected. This series of ions indicated that glycine is located in the inner core region of the LOS in *C. jejuni* GB19. To define more precisely its position, the ion at *m*/*z* 961.3 was further fragmented in a MS^3 experiment. The product ion spectrum is shown in Figure 4C, in which Y-type ions at *m*/*z* 434.4, 596.5, and 799.2 correspond to compositions $[Hex_1{\cdot}Hep_1{\cdot}Gly + Na]^+$, $[HexNAc_1{\cdot}Hex_1{\cdot}Hep_1{\cdot}Gly + Na]^+$, and $[HexNAc_1{\cdot}Hex_2{\cdot}Hep_1{\cdot}Gly + Na]^+$, respectively. These fragment ions indicated that the glycine residue could substitute Hex or Hep. Tandem MS experiments on the protonated parent ions were therefore performed for Gly-substituted and non-Gly-substituted glycoforms (Figure 4D). By comparing the two MS^2 spectra, we can conclude that the Gly substitutes for Hep and not Hex. Similar results were observed for *C. jejuni* strains MF6, GB16, GB26, and GC033 (data not shown). Therefore, the fragment ion at *m*/*z* 250.1 of the protonated parent ion can be used as a diagnostic ion to detect glycinated species in strains that adopt a structure consistent with core 2 in Scheme 1.

Three other strains (GB11, ATCC 43446, and OH4384) share the same core LOS structure (core 3 in Scheme 1). The tandem spectra indicate that this amino acid is also localized to Hep_{II} (Supporting Information, Figure S2). The fragment ion at *m*/*z* 799.3 of the sodiated parent ion, together with the fragment ion at *m*/*z* 250.1 of the protonated parent ion, can therefore be used as the diagnostic ion for strains that adopt the second structure presented in Scheme 1. Similar analysis was performed for strains OH4382, HB93-13, and GC175 (Supporting Information, Figure S3) for which the LOS has a structure represented by core 4 (Scheme 1). The results demonstrate once again that glycine was localized to Hep_{II}.

DISCUSSION

LOS is a virulence factor of *C. jejuni* and is involved in the development of post-infectious neuropathies, due to molecular mimicry between the LOS core structure and ganglioside epitopes on peripheral nerve tissue. Structural

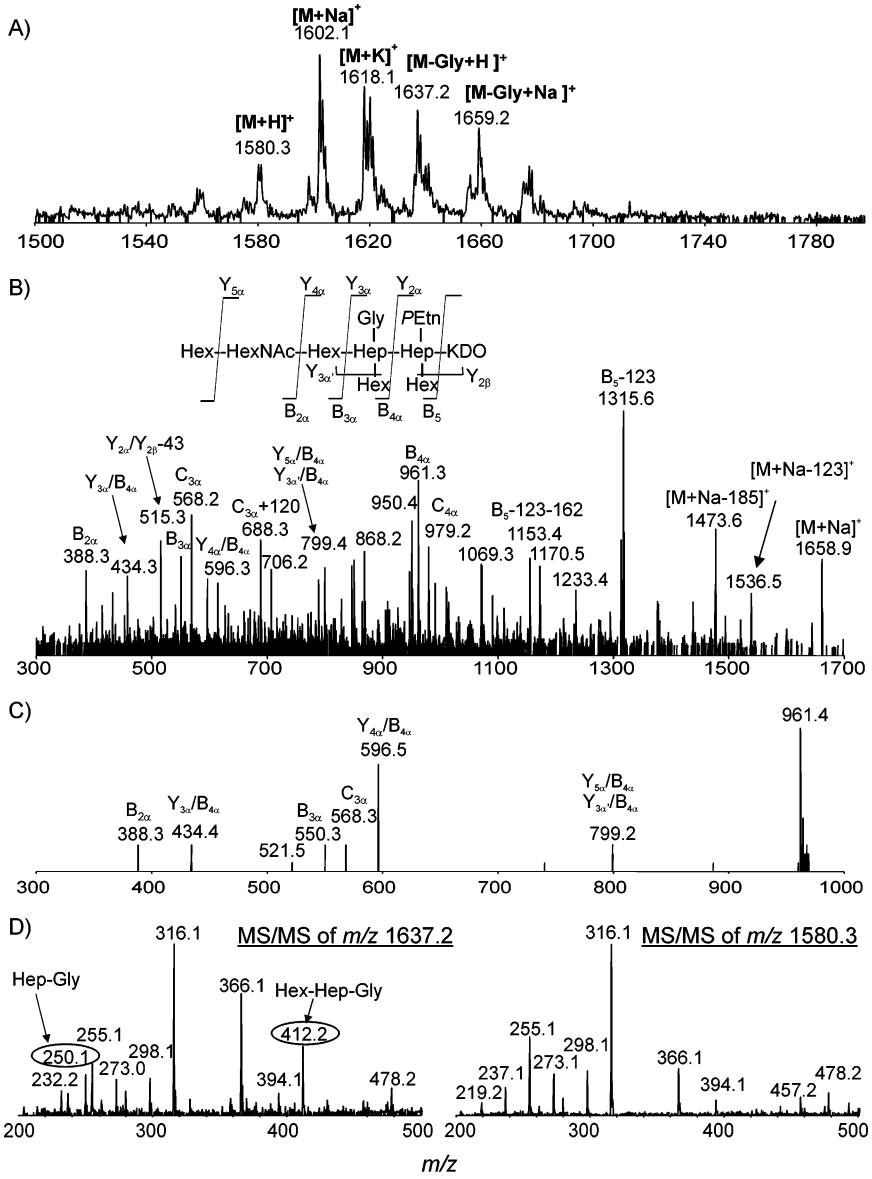

FIGURE 4: MS and MS/MS analysis of core oligosaccharides of *C. jejuni* GB19. (A) Extracted MS spectrum. (B) Extracted MS/MS spectrum of the ion at *m*/*z* 1659.2 ($[M + Na]^+$), corresponding to a composition of Gly·Hex_4·$HexNAc_1$·Hep_2·*P*Etn_1·KDO_1. (C) Extracted MS^3 spectrum of the ion at *m*/*z* 961.4 ($[M + Na]^+$, produced from *m*/*z* 1659.2). (D) Extracted MS/MS spectra of protonated ions at *m*/*z* 1637.2 and 1580.3, corresponding to compositions of Gly·Hex_4·$HexNAc_1$·Hep_2·*P*Etn_1·KDO_1 and Hex_4·$HexNAc_1$·Hep_2·*P*Etn_1·KDO_1, respectively. The fragment ions are assigned according to the nomenclature of Domon and Costello (*34*).

studies have shown that many *C. jejuni* strains have LOS-containing ganglioside-like structures with sialic acid as an essential appendage (*13*). The LOSs in some of the *C. jejuni* strains investigated in this study contain up to three sialic acid residues, linked terminally and/or subterminally to galactose. MS spectra of intact LOS from *C. jejuni* strains provided information about the structure and relative distribution of specific species within the ensemble of glycoforms. A quick profiling of LOS glycoforms was performed using precursor ion scan experiments to screen for the presence of specific glycoforms in a complex mixture. The selective ion scanning for *m*/*z* 290.1, specific for Neu5Ac residues, and *m*/*z* 581.2, specific for Neu5Ac-Neu5Ac, suggested the presence of monosialylated and disialylated glycoforms, respectively. Monosialylated LOSs were the major glycoforms in *C. jejuni* strains predicted to have a monofunctional Cst-II variant (or Cst-III) and include ATCC 43446, GB11, GB26, GC175, and NCTC 11168. Strains GB26, GC175, and NCTC 11168 had a single Neu5Ac residue in their LOS. ATCC 43446 and GB11 had glycoforms with either one or two mono-Neu5Ac forms, with the inner Gal residue always substituted and the terminal Gal residue variably substituted (see the scheme in the Supporting Information). Disialylated (Neu5Ac-Neu5Ac) populations of LOS glycoforms have been detected in the strains predicted to have a bifunctional Cst-II and include MF6, GB16, GB19, OH4382, HB93-13, and GC033. Trace amounts of disialylated (Neu5Ac-Neu5Ac) populations of LOS glycoforms were also observed in ATCC 43446 and GB11, even though these strains are predicted to contain monofunctional Cst-II variants. Tandem mass spectrometric studies of intact LOS from *C. jejuni* strain OH4384 showed evidence of the existence of monosialic acid and a disialic acid attached to different sugar residues.

Sialic acids in the LOS of *C. jejuni* can be modified with *O*-acetyl groups. We have previously confirmed by NMR experiments the existence of an enzyme (SOAT) in *C. jejuni*,

which *O*-acetylates carbohydrate-bound Neu5Ac (*25*). However, we were only able to detect *O*-acetylated Neu5Ac after it was released from the cells by a neuraminidase. We could not directly demonstrate the presence of LOS-bound *O*-acetylated Neu5Ac by MS, because sample preparation involved an *O*-deacylation step, which is commonly used to remove *O*-linked fatty acid chains but also removes O-linked acetate. Using an EA-OTLC−MS strategy to analyze intact LOS, we were able to obtain direct evidence of the presence of LOS-bound *O*-acetylated sialic acids. While MS spectra were able to show the presence of *O*-acetylated sialic acids, tandem mass spectrometry provided much more confident structural information for highly complicated spectra. Therefore, we employed precursor ion scan experiments to probe for Neu5Ac *O*-acetylation. A quick profiling of LOS glycoforms for the existence of *O*-acetyl-Neu5Ac and *O*-acetyl-Neu5Ac-Neu5Ac was achieved by using precursor ions at *m*/*z* 332.1 and 622.2, respectively. The *O*-acetylated Neu5Ac-containing glycoforms were detected in strains MF6, GB16, GB19, HB93-13, and GC033, all of which contain both predicted SOAT and bifunctional Cst-II activities. Trace amounts of *O*-acetylated Neu5Ac-containing glycoforms were also detected in strains ATCC 43446 and GB11 (see below).

The presence of both an active SOAT and a bifunctional Cst-II is required for the expression of *O*-acetylated Neu5Ac in the LOS outer core. The strains used in this study were selected to encompass several possible combinations comprising active or inactive versions of the SOAT and mono- or bifunctional copies of Cst-II. The predicted phenotypes correlate perfectly with the presence or absence of *O*-acetylated Neu5Ac, except for ATCC 43446 and GB11, which we found to contain trace amounts of *O*-acetylated Neu5Ac. This was surprising since these strains were thought to possess monofunctional versions of Cst-II (see above). On the basis of MS analysis presented in this work, we can now confirm that they express small quantities of disialylated glycoforms that serve as targets for *O*-acetylation. The sialyltransferase carried by these strains appears to possess very low levels of α2−8-transferase activity.

The characterized strains were also selected to represent various clinical presentations (Table 2). GBS, an immune-mediated neuropathy, and its variant FS are rare but serious post-infectious complications of *C. jejuni* infection. Most patients with *C. jejuni*-associated GBS have high titers of antibodies to various gangliosides in their acute-phase sera (*5*). The presence of specific anti-ganglioside antibodies strongly correlates with the clinical presentation (*5*). Frequently, these antibodies cross-react with the LOS of the associated *C. jejuni* strain; therefore, the elucidation of the outer core structure can provide a structural basis for the clinical presentation. Among the five strains found to contain high levels of *O*-acetylated Neu5Ac, two (MF6 and GC033) were isolated from patients with FS, which is characterized by oculomotor weakness and ataxia. Two (GB16 and GB19) came from GBS patients who also had ocular symptoms (*8*). The other strain (HB93-13) with *O*-acetylated Neu5Ac came from a patient with the axonal form of GBS, without ocular symptoms (*35*). In summary, four of the five patients with some ocular symptoms had *C. jejuni* strains with *O*-acetylated Neu5Ac in their LOSs. We note, however, that this association may be strongly correlated with the fact that these strains also express disialate residues, which can trigger anti-GQ1b antibodies and are implicated in the pathology of these conditions. FS is strongly associated with the presence of anti-GQ1b antibodies (*36*). The significance of *O*-acetylated Neu5Ac in clinical presentations will be clearer upon examination of a large set of *C. jejuni* strains. Our ability to use MS approaches to characterize small quantities of material will facilitate this task.

The presence of *O*-linked glycine residues in *C. jejuni* LOS has not been reported previously, due to the *O*-deacetylation preparation procedure. Almost all *C. jejuni* strains investigated in our study express *O*-glycine substituents in their inner core oligosaccharide regions. Interestingly, *C. jejuni* 11168 is the only strain in which we did not detect glycine modification. However, we could not determine if the gene responsible for adding glycine is absent or inactive. To locate the glycine residue in the inner core oligosaccharide, MS/MS experiments were performed in positive ion mode on core oligosaccharide samples. The results revealed that glycine was located on the distal heptose residue (Hep_{II}) for each strain. Structural information about the linkage of glycine residue is being sought.

SUPPORTING INFORMATION AVAILABLE

Analysis of intact LOSs from a single-colony extract from strain MF6 (Figure S1) and, for the purpose of localizing glycine, tandem mass spectrometry characterization of the LOSs in strains GB11, ATCC 43446, and OH4384 (Figure S2) and strains OH4382, HB93-13, and GC175 (Figure S3). This material is available free of charge via the Internet at http://pubs.acs.org.

REFERENCES

1. Godschalk, P. C., Heikema, A. P., Gilbert, M., Komagamine, T., Ang, C. W., Glerum, J., Brochu, D., Li, J., Yuki, N., Jacobs, B. C., van Belkum, A., and Endtz, H. P. (2004) The crucial role of *Campylobacter jejuni* genes in autoimmune antibody induction, *J. Clin. Invest. 114*, 1659−1665.
2. Allos, B. M. (2001) *Campylobacter jejuni* infections: Update on emerging issues and trends, *Clin. Infect. Dis. 32*, 1201−1206.
3. Public Health Agency of Canada (2006) Canada communicable disease report. http://dsol-smed.phac-aspc.gc.ca/dsol-smed/indis/index_e.html.
4. Yuki, N., Yoshino, H., Sato, S., and Miyatake, T. (1990) Acute axonal polyneuropathy associated with anti-GM1 antibodies following *Campylobacter* enteritis, *Neurology 40*, 1900−1902.
5. Yuki, N. (2001) Infectious origins of, and molecular mimicry in, Guillain-Barré and Fisher syndromes, *Lancet Infect. Dis. 1*, 29−37.
6. Yuki, N. (2007) Ganglioside mimicry and peripheral nerve disease, *Muscle Nerve 35*, 691−711.
7. Nachamkin, I., Allos, B. M., and Ho, T. (1998) *Campylobacter* species and Guillain-Barré syndrome, *Clin. Microbiol. Rev. 11*, 555−567.
8. Godschalk, P. C., Kuijf, M. L., Li, J., St Michael, F., Ang, C. W., Jacobs, B. C., Karwaski, M. F., Brochu, D., Moterassed, A., Endtz, H. P., van Belkum, A., and Gilbert, M. (2007) Structural characterization of *Campylobacter jejuni* lipooligosaccharide outer cores associated with Guillain-Barré and Miller Fisher syndromes, *Infect. Immun. 75*, 1245−1254.
9. Jacobs, B. C., Endtz, H., van der Meche, F. G., Hazenberg, M. P., Achtereekte, H. A., and van Doorn, P. A. (1995) Serum anti-GQ1b IgG antibodies recognize surface epitopes on *Campylobacter jejuni* from patients with Miller Fisher syndrome, *Ann. Neurol. 37*, 260−264.
10. Moran, A. P., Scholz, D., and Zähringer, U. (1992) Application of methylation analysis in the determination of the structure of

disaccharides containing 2,3-diamino-2,3-dideoxy-D-glucose (GlcN3N) associated with the backbone of lipid A, *Carbohydr. Res. 231*, 309−316.
11. Moran, A. P., Zähringer, U., Seydel, U., Scholz, D., Stutz, P., and Rietschel, E. T. (1991) Structural analysis of the lipid A component of *Campylobacter jejuni* CCUG 10936 (serotype O:2) lipopolysaccharide. Description of a lipid A containing a hybrid backbone of 2-amino-2-deoxy-D-glucose and 2,3-diamino-2,3-dideoxy-D-glucose, *Eur. J. Biochem. 198*, 459−469.
12. Aspinall, G. O., McDonald, A. G., Raju, T. S., Pang, H., Kurjanczyk, L. A., Penner, J. L., and Moran, A. P. (1993) Chemical structure of the core region of *Campylobacter jejuni* serotype O:2 lipopolysaccharide, *Eur. J. Biochem. 213*, 1029−1037.
13. Aspinall, G. O., McDonald, A. G., Pang, H., Kurjanczyk, L. A., and Penner, J. L. (1994) Lipopolysaccharides of *Campylobacter jejuni serotype* O:19: structures of core oligosaccharide regions from the serostrain and two bacterial isolates from patients with the Guillain-Barré syndrome, *Biochemistry 33*, 241−249.
14. Guerry, P., Ewing, C. P., Hickey, T. E., Prendergast, M. M., and Moran, A. P. (2000) Sialylation of lipooligosaccharide cores affects immunogenicity and serum resistance of *Campylobacter jejuni*, *Infect. Immun. 68*, 6656−6662.
15. Prendergast, M. M., Lastovica, A. J., and Moran, A. P. (1998) Lipopolysaccharides from *Campylobacter jejuni* O:41 strains associated with Guillain-Barré syndrome exhibit mimicry of GM1 ganglioside, *Infect. Immun. 66*, 3649−3655.
16. Salloway, S., Mermel, L. A., Seamens, M., Aspinall, G. O., Nam Shin, J., Kurjanczyk, E., and Penner, J. L. (1996) Miller Fisher syndrome associated with *Campylobacter jejuni* bearing lipopolysaccharide molecules that mimic human ganglioside GD3, *Infect. Immun. 64*, 2945−2949.
17. Aspinall, G. O., McDonald, A. G., Raju, T. S., Pang, H., Moran, A. P., and Penner, J. L. (1993) Chemical structures of the core regions of *Campylobacter jejuni* serotypes O:1, O:4, O:23 and O:36 lipopolysaccharides, *Eur. J. Biochem. 213*, 1017−1027.
18. Gilbert, M., Karwaski, M.-F., Bernatchez, S., Young, N. M., Taboada, E., Michniewicz, J., Cunningham, A.-M., and Wakarchuk, W. W. (2002) The genetic bases for the variation in the lipooligosaccharide of the mucosal pathogen, *Campylobacter jejuni*. Biosynthesis of sialylated ganglioside mimics in the core oligosaccharide, *J. Biol. Chem. 277*, 327−337.
19. Chiu, C. P. C., Watts, A. G., Lairson, L. L., Gilbert, M., Lim, D., Wakarchuk, W. W., Withers, S. G., and Strynadka, N. C. J. (2004) Structural analysis of the sialyltransferase CstII from *Campylobacter jejuni* in complex with a substrate analog, *Nat. Struct. Mol. Biol. 11*, 163−170.
20. Schauer, R. (1991) Biosynthesis and function of *N*- and *O*-substituted sialic acids, *Glycobiology 1*, 449−452.
21. Varki, A. (1992) Diversity in the sialic acids, *Glycobiology 2*, 25−40.
22. Lewis, A. L., Nizet, V., and Varki, A. (2004) Discovery and characterization of sialic acid *O*-acetylation in group B *Streptococcus*, *Proc. Natl. Acad. Sci. U.S.A. 101*, 11123−11128.
23. Carlin, A. F., Lewis, A. L., Varki, A., and Nizet, V. (2007) Group B streptococcal capsular sialic acids interact with siglecs (immunoglobulin-like lectins) on human leukocytes, *J. Bacteriol. 189*, 1231−1237.
24. Deszo, E. L., Steenbergen, S. M., Freedberg, D. I., and Vimr, E. R. (2005) *Escherichia coli* K1 polysialic acid *O*-acetyltransferase gene, *neuO*, and the mechanism of capsule form variation involving a mobile contingency locus, *Proc. Natl. Acad. Sci. U.S.A. 102*, 5564−5569.
25. Houliston, R. S., Endtz, H. P., Yuki, N., Li, J., Jarrell, H. C., Koga, M., van Belkum, A., Karwaski, M.-F., Wakarchuk, W. W., and Gilbert, M. (2006) Identification of a sialate *O*-acetyltransferase from *Campylobacter jejuni*: Demonstration of direct transfer to the C-9 position of α-2,8-linked sialic acid, *J. Biol. Chem. 281*, 11480−11486.
26. Li, J., Koga, M., Brochu, D., Yuki, N., Chan, K., and Gilbert, M. (2005) Electrophoresis-assisted open-tubular liquid chromatography/mass spectrometry for the analysis of lipooligosaccharide expressed by *Campylobacter jejuni*, *Electrophoresis 26*, 3360−3368.
27. Takahashi, M., Koga, M., Yokoyama, K., and Yuki, N. (2005) Epidemiology of *Campylobacter jejuni* isolated from patients with Guillain-Barré and Fisher syndromes in Japan, *J. Clin. Microbiol. 43*, 335−339.
28. Ahmed, I. H., Manning, G., Wassenaar, T. M., Cawthraw, S., and Newell, D. G. (2002) Identification of genetic differences between two *Campylobacter jejuni* strains with different colonization potentials, *Microbiology 148*, 1203−1212.
29. Parkhill, J., Wren, B. W., Mungall, K., Ketley, J. M., Churcher, C., Basham, D., Chillingworth, T., Davies, R. M., Feltwell, T., Holroyd, S., Jagels, K., Karlyshev, A. V., Moule, S., Pallen, M. J., Penn, C. W., Quail, M. A., Rajandream, M. A., Rutherford, K. M., van Vliet, A. H., Whitehead, S., and Barrell, B. G. (2000) The genome sequence of the food-borne pathogen *Campylobacter jejuni* reveals hypervariable sequences, *Nature 403*, 665−668.
30. Gamian, A., Mieszala, M., Katzenellenbogen, E., Czarny, A., Zal, T., and Romanowska, E. (1996) The occurrence of glycine in bacterial lipopolysaccharides, *FEMS Immunol. Med. Microbiol. 13*, 261−268.
31. Cox, A. D., Li, J., and Richards, J. C. (2002) Identification and localization of glycine in the inner core lipopolysaccharide of *Neisseria meningitidis*, *Eur. J. Biochem. 269*, 4169−4175.
32. Li, J., Bauer, S. H. J., Månsson, M., Moxon, E. R., Richards, J. C., and Schweda, E. K. H. (2001) Glycine is a common substituent of the inner core in *Haemophilus influenzae* lipopolysaccharide, *Glycobiology 12*, 1009−1015.
33. Yildirima, H. H., Li, J., Richards, J. C., Hood, D. W., Moxon, E. R., and Schweda, E. K. H. (2005) Complex *O*-acetylation in nontypeable *Haemophilus influenzae* lipopolysaccharide: Evidence for a novel site of *O*-acetylation, *Carbohydr. Res. 340*, 2598−2611.
34. Domon, B., and Costello, C. E. (1988) A systematic nomenclature for carbohydrate fragmentations in FAB-MS/MS spectra of glycoconjugates, *Glycoconjugate J. 5*, 397−409.
35. Sheikh, K. A., Nachamkin, I., Ho, T. W., Willison, H. J., Veitch, J., Ung, H., Nicholson, M., Li, C. Y., Wu, H. S., Shen, B. Q., Cornblath, D. R., Asbury, A. K., McKhann, G. M., and Griffin, J. W. (1998) *Campylobacter jejuni* lipopolysaccharides in Guillain-Barré syndrome: Molecular mimicry and host susceptibility, *Neurology 51*, 371−378.
36. Chiba, A., Kusunoki, S., Obata, H., Machinami, R., and Kanazawa, I. (1993) Serum anti-GQ1b IgG antibody is associated with ophthalmoplegia in Miller Fisher syndrome and Guillain-Barré syndrome: Clinical and immunohistochemical studies, *Neurology 43*, 1911−1917.

BI701229K